



LAWRENCE
LIVERMORE
NATIONAL
LABORATORY

Extrinsic Paramagnetic Meissner Effect in Multiphase Indium-Tin Alloys

S. Chu, A. J. Schwartz, T. B. Massalski, D. E. Laughlin

December 6, 2005

Nature

Disclaimer

This document was prepared as an account of work sponsored by an agency of the United States Government. Neither the United States Government nor the University of California nor any of their employees, makes any warranty, express or implied, or assumes any legal liability or responsibility for the accuracy, completeness, or usefulness of any information, apparatus, product, or process disclosed, or represents that its use would not infringe privately owned rights. Reference herein to any specific commercial product, process, or service by trade name, trademark, manufacturer, or otherwise, does not necessarily constitute or imply its endorsement, recommendation, or favoring by the United States Government or the University of California. The views and opinions of authors expressed herein do not necessarily state or reflect those of the United States Government or the University of California, and shall not be used for advertising or product endorsement purposes.

Extrinsic Paramagnetic Meissner Effect in Multiphase Indium-Tin Alloys

Shaoyan Chu^{1,3}, Adam J. Schwartz², Thaddeus B. Massalski¹ and David E. Laughlin¹

¹ Department of Materials Science and Engineering, Carnegie Mellon University, Pittsburgh, PA 15213

² Physics and Advanced Technologies Directorate, Lawrence Livermore National Laboratory, Livermore, California 94550, USA

³ Center for Materials Science and Engineering, Massachusetts Institute of Technology, 77 Massachusetts Avenue, Cambridge, MA 02139.

A well-known effect in superconducting materials below their critical temperatures (T_c) is the reduction to zero of their electrical resistivities. Concomitantly, the materials become perfect diamagnets for small fields. This effect, termed the Meissner Effect, allows for the direct measurement of the transition temperature (T_c) by magnetic techniques such as the superconducting quantum interference device (SQUID). A Paramagnetic Meissner Effect (PME), i.e., the unexpected observation of positive magnetic moment in a superconductor below its critical temperature during field cooling (FC), was first reported in 1989 by Svedlindh *et al.* (1). The origin of PME in high T_c superconductors has been discussed by numerous investigators as possibly resulting from π -junctions, d-wave behavior, giant vortex states, flux compression, or weak links. In conventional superconductors like Nb, the PME was ascribed to the inhomogeneous nature of such samples, whereby their surface is sufficiently different from the interior and becomes superconducting at a higher temperature than the interior on cooling, thereby trapping the magnetic flux. There remains significant controversy regarding the fundamental origin of the PME. Here, we show that the PME in two-phase and three-phase In-Sn alloys is a property resulting from the morphological distribution of the multiple phases. We propose that PME in these alloys results from microstructural encapsulation of the grains of one superconducting phase inside the grains of another (e.g., the matrix) which has a higher T_c . Hence the PME in this case is *extrinsic* in nature rather than *intrinsic* to the material, and could be described as an Extrinsic Paramagnetic Meissner Effect (EPME). It may be expected to occur in multiple-phase alloy samples where more than one of the phases is superconducting, or in nominally single-phase materials where the surface of the specimen, grain boundaries, or other defects have different superconducting properties. This discovery opens the possibility of being able to control the EPME for potential applications in supercomputers, radiation detection, and sensors.

We have been investigating the low temperature phase transformations in In-Sn alloys. The extended phase diagram for these alloys is shown in Figure 1 (2). Although in this diagram the metallic β -Sn phase is shown to be stable at temperatures above the room temperature, in practice it remains metastable also at cryogenic temperatures. Each of the phases, β -Sn, γ -InSn, and β -InSn becomes superconducting at low temperatures (~ 3.8 K,

~4.7K, and ~6.2K, respectively) and hence their presence and the amount present can be detected by SQUID magnetometer measurements. Because these phases are stable (or metastable) over a range of compositions at low temperatures, their superconducting transition temperatures are a function of the particular compositions, or composition ranges of each of the phases, and thus varies with the processing conditions of the sample. In the course of investigating a $\text{In}_{10}\text{Sn}_{90}$ alloy that contained the β -Sn phase in the γ -InSn matrix we observed the Paramagnetic Meissner Effect behavior. The particular arrangement of the two phases in the $\text{In}_{10}\text{Sn}_{90}$ alloy is the result of a low temperature phase transformation (γ -InSn $\rightarrow\beta$ -Sn) which occurs by a martensitic, or displacive mechanism (3). This compositionally invariant shear transformation produces a microstructure in which the β -Sn particles are contained within (i.e., encapsulated) in the γ -In-Sn matrix. Upon cooling through the superconducting transition temperature of the γ -InSn, at approximately 4.7K, the matrix will exclude the magnetic flux and thus compress some of the flux inside the β -Sn particles, thus inducing the paramagnetic response, as shown in the magnetic moment versus temperature plot in Figure 2. Here, on cooling with an imposed magnetic field, the γ phase becomes superconducting at approximately 4.8K. It is important to point out that neither the pure β -Sn phase nor the pure γ -InSn phase show this effect. It occurs only when there is a mixture of phases. Thus, we believe that the observed paramagnetic response behavior in our In-Sn alloy is the result of the specific microstructure of this alloy. That is, we believe that the PME in our alloys is an extrinsic effect in nature, involving two interacting phases rather than intrinsic to a one-phase material.

To test the hypothesis of the extrinsic nature of PME, we constructed a sample with a core of β -Sn, an outside shell of a β -InSn alloy (20 at.%Sn) and an intermediate shell of the γ -InSn phase. The samples were prepared by melting a $\text{In}_{80}\text{Sn}_{20}$ alloy specimen with a melting temperature of ~423K around a rod of pure β -Sn under vacuum in a quartz tube. While the β -InSn alloy was molten, a small amount of interdiffusion occurred, such that In diffused into the β -Sn phase, reacting to form a thin ring of the γ -InSn phase between the β -InSn alloy and β -Sn. A schematic cross-section of the sample is shown in Figure 3a along with an optical macrograph in Figure 3b, including a composition profile. The composition profile were determined with wavelength dispersive spectroscopy in a scanning electron microscope. For the SQUID measurements, a 4 mm diameter disk with a thickness of 0.7 mm was prepared from a section of the solidified composite alloy rod. The magnetic field was applied perpendicular to the flat faces of the sample. The composition profile reveals that the β -Sn phase has a uniform composition. The γ -InSn phase exhibits a composition variation with In contents between ~75 and 85% Sn as expected from the equilibrium phase diagram. The composition of the β -InSn alloy reveals only minor Sn fluctuations. From these composition profiles, we would expect that the β -Sn and β -InSn phases should exhibit well-defined critical temperatures. However, due to the smoothly changing composition profile within the γ -InSn phase, we may expect that the superconducting transition temperature in this phase will occur over a range of temperatures.

The field cooling results of our “manufactured” sample are shown in Figure 4. There are clear breaks in the curve at temperatures (6.2 and 3.8 K) corresponding to the superconducting transition temperatures of β -InSn and β -Sn respectively. The increase in magnetic moment at 4.7 K is less distinct and corresponds to the critical temperature of the compositionally-varying γ -InSn phase. At 6.2 K the outside phase (β -InSn) becomes superconducting (and hence diamagnetic) and traps the applied field within the inner core of the sample when the magnetic field is perpendicular to the sample cross-section. This is the cause of the positive measured value for the magnetic moment of the sample (PME). The next phase (γ -InSn) becomes superconducting at 4.7 K and this is displayed in the figure as well and further compresses the flux in the β -Sn inner disk. Finally, the β -Sn phase core becomes superconducting at 3.8 K and excludes the magnetic flux, giving rise to a drop in the magnetic moment.

As we noted earlier, the first observation of an increase in magnetization of a sample upon cooling through the critical temperature was reported by Svedlindh et al. (1) while studying a high temperature superconductor $\text{Bi}_2\text{Sr}_2\text{Ca}_1\text{Cu}_2\text{O}_{8+\delta}$. Later, Braunisch et al. (4, 5), while studying a similar nominal sample of $\text{Bi}_2\text{Sr}_2\text{Ca}_1\text{Cu}_2\text{O}_{8+\delta}$ also reported this 'striking' paramagnetism, which they called a Paramagnetic Meissner Effect (PME). The majority of authors who reported PME thereafter in a variety of superconductor materials recognized that some defects, or proximity effects, must be involved in the superconductor sample. Some authors also point out that not all measured samples of the same nominal composition material exhibit the PME (6). Attempts to develop a more fundamental understanding of this "anti-Meissner" phenomenon, range from proposed networks of Josephson-junctions (7-9) coupled with π -junctions (10, 11), various forms of flux compression (6, 12-16), and various forms of sample microstructural effects, including structural defects (17-21).

Interpretations of PME observed in essentially pure materials such as Nb-discs (16, 21), Al-discs (22), etc., all imply that different portions of a given sample may exhibit subtle differences in the values of T_c , particularly on the surface, and the way in which the magnetic flux is expelled, compressed, or trapped. Our present experiments indicate that PME can be shown to be an extrinsic phenomenon requiring the presence of different phases with different T_c values, and requiring a specific spatial distribution of such phases within the sample.

Thus, in our samples, the PME is clearly a microstructural phenomenon; that is it is caused by the specific geometry of the phases present. Such a feature is expected whenever multiple superconducting phases coexist in an alloy in such a way that the phase with a lower transition temperature is surrounded by a phase, or phases, with a higher transition temperature(s). This proposed mechanism is somewhat like the explanation of Kostic et al. (16) for the PME in Nb, where the surface of the Nb was considered to be a different phase with a higher superconducting transition temperature.

We therefore propose that whenever the PME is observed in a multiphase sample (or one in which defects may act to resemble a multiphase sample) this Extrinsic Paramagnetic Meissner Effect (EPME) should be considered as a possible explanation. The

understanding how EPME arises in multiphase samples should allow the production of EPME at will rather than as an artifact of sample preparation.

Acknowledgments

This work was performed under the auspices of U.S. Department of Energy by the University of California, Lawrence Livermore National Laboratory under contract No. W-7405-Eng-48.

1. Svedlindh, P. et al. Anti-Meissner effect in the BiSrCaCuO-System. *Physica C*, **162-164**, 1365-1366 (1989).
2. Massalski, T. B. et al. Binary Alloy Phase Diagrams, second edition, American Society for Metals, 1990.
3. Chu, S. et al. Low Temperature Phase Instability of the Gamma Phase in InSn Alloys, in press, **Solid-Solid Phase Transformations in Inorganic Materials, TMS 2005**.
4. Braunisch, W. et al. Paramagnetic Meissner effect in Bi high-temperature superconductors. *Phys. Rev. Lett.* **68**, 1908-1911 (1992).
5. Braunisch, W. et al. Paramagnetic Meissner effect in high-temperature superconductors, *Physical Review B*, **48**, 4030-4042 (1992).
6. Okram, G. S., Adroja, D. T., Padalia, B. D., Prakash, O. & de Groot, P. A. J. The paramagnetic Meissner effect in Nd_{2-x}Ce_xCuO_y superconductors at 40 G and flux trapping. *J. Phys.: Condens. Matter*, **9**, L525-L531 (1997).
7. Sigrist, M. & Rice, T. M. Paramagnetic effect in High-TC superconductors – a hint for d-wave superconductivity. *J. Phys. Soc. Jpn* **61**, 4283-4286 (1992).
8. Dias, R. T., Pureur, P., Rodrigues, Jr., P. & Obradors, X. Paramagnetic effect at low and high magnetic field in melt-textured YBa₂Cu₃O_{7-δ}. *Physical Review B*, **70**, 224519 (2004).
9. Nielsen A.P. et al. Paramagnetic meissner effect in multiply-connected superconductors. *Physical Review B*, **62**, 14380-14383 (2000).
10. Dominguez, D., Jagla, E. A. & Balseiro, C. A. Phenomenological theory of the paramagnetic Meissner effect. *Phys. Rev. Lett.* **72**, 2773-2776 (1994).
11. Magnusson, J. et al. Time-dependence of the magnetization of BiSrCaCuO displaying the paramagnetic Meissner effect. *Phys. Rev. B* **52**, 7675-7681 (1995).
12. Koshelev, A. E. & Larkin, A. I. Paramagnetic moment in field-cooled superconducting plates: paramagnetic Meissner effect. *Phys. Rev. B* **52**, 13559-13562 (1995).
13. Moshchalkov, V. V., Qui, X. G. & Bruyndoncz, V. Paramagnetic Meissner effect from the selfconsistent solution of the Ginzburg-Landau equations. *Phys. Rev. B* **55**, 11793-11801 (1997).
14. Zhu, B-H., Zhou, S-P., Zha, G-Q. & Yang, K. Charge distributions due to paramagnetism and diamagnetism in thin mesoscopic superconducting rings. *Physics Letters A*. **338**, 420-424 (2005).
15. Pust L., Wenger, L. E. & Koblishka, M. R. Detailed investigation of the superconducting transition of niobium disks exhibiting the paramagnetic Meissner effect. *Physical Review B*, **58**, 14191-14194 (1998).

16. Kostic, P. et al. Paramagnetic Meissner effect in Nb. *Phys. Rev. B* **53**, 791-801 (1996).
17. Riedling, S. et al. Observation of the Wohlleben effect in YBaCuO single crystals. *Phys. Rev. B* **49**, 13283-13286 (1994).
18. Khalil, A. E. Inversion of Meissner effect and granular disorder in BiSrCaCuO superconductors. *Phys. Rev. B* **55**, 6625-6630 (1997).
19. Ortiz, W. A., Lisboa-Filho, P. N., Passos, W. A. C. & Araujo-Moreira, F. M. Field-induced networks of weak-links: an experimental demonstration that the paramagnetic Meissner effect is inherent to granularity. *Physica C*, **361**, 267-273 (2001).
20. Heinzl, C., Theilig, T. & Ziemann, P. Paramagnetic Meissner effect analyzed by second harmonics of the magnetic susceptibility: Consistency with a ground state carrying spontaneous currents. *Phys. Rev. B* **48**, 3445-3454 (1993).
21. Fodor, P. S. & Wenger, L. E. Paramagnetic Meissner effect in Nb disks. *Physica C* **341-348**, 2043-2044 (2000).
22. Geim, A. K., Dubonos, S. V., Lok, J. G. S., Henini, M. & Maan, J. C. Paramagnetic Meissner effect in small superconductors. *Nature* **396**, 144-146 (1998).

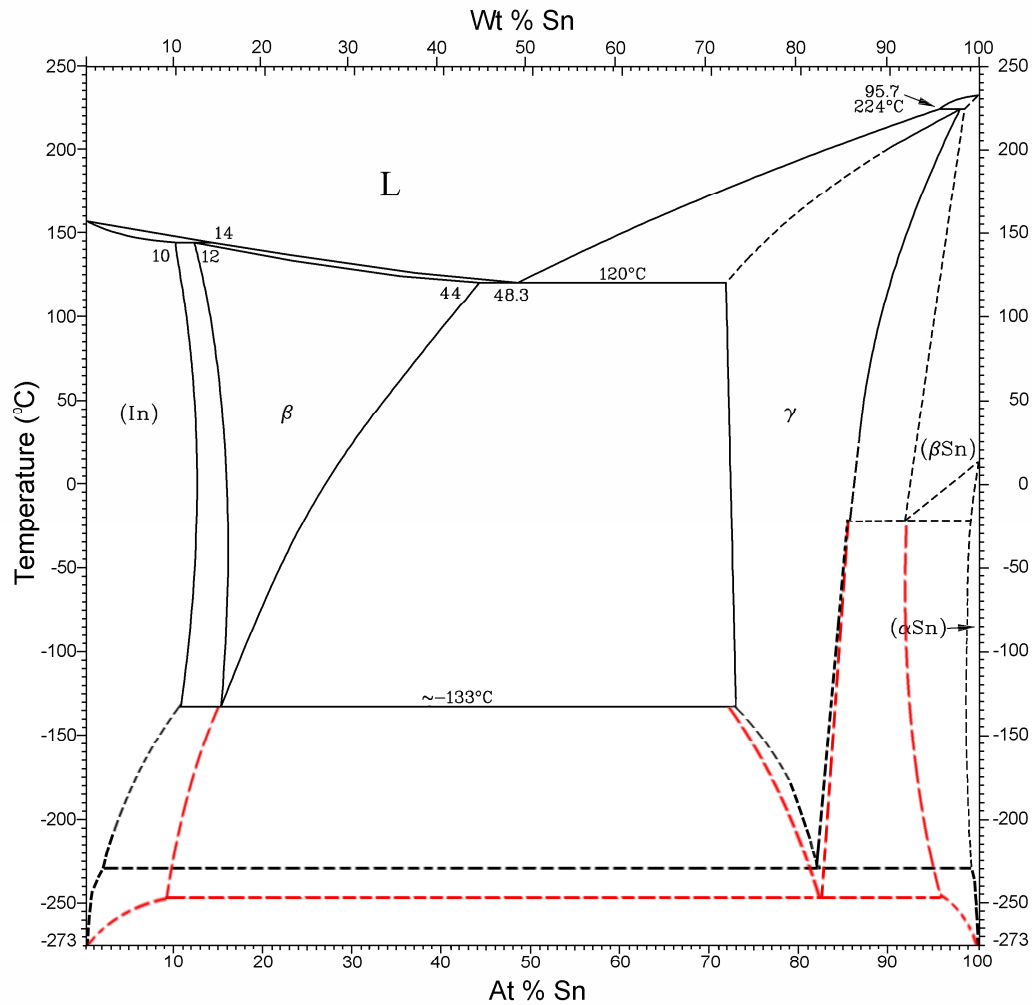


Figure 1. Phase diagram of the system InSn (2) and possible metastable phase extensions at low temperatures based on observed phase transformations (3) The three phases of interest in this investigation are β -Sn (bct, tI4), γ -InSn (sh, hP1), and β -InSn (bct, tI2) with superconducting transition temperatures of ~ 5.5 - 6.5 , ~ 6.0 - 4.2 and 3.7 K respectively,

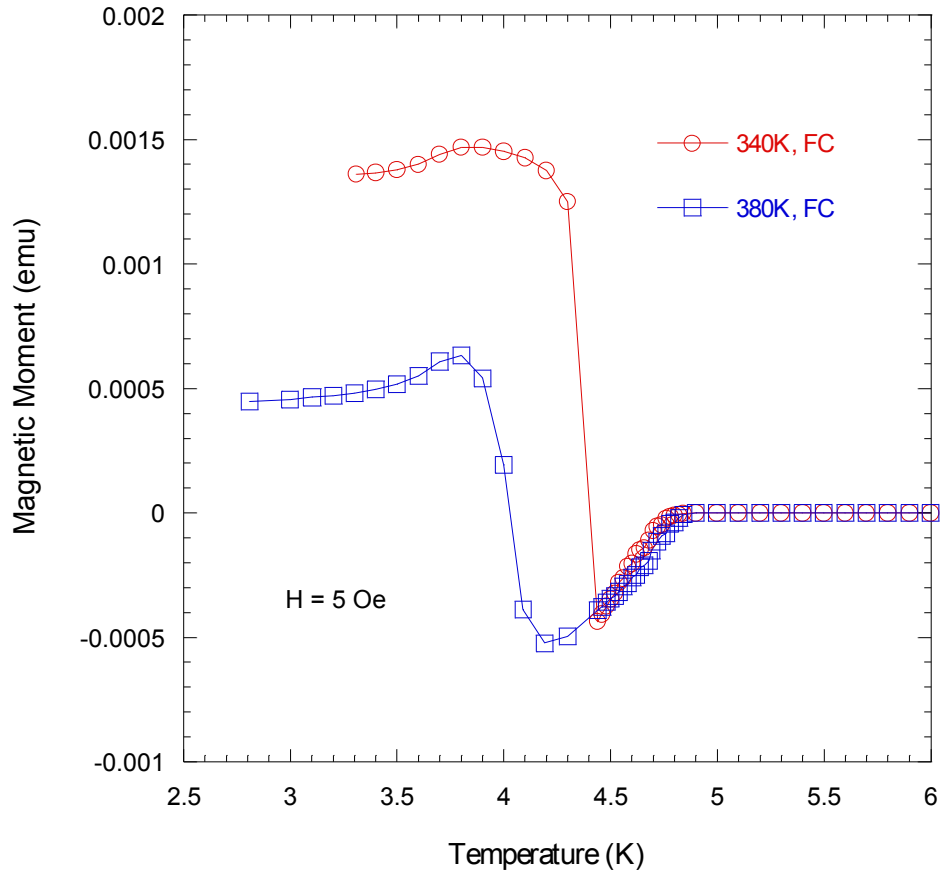


Figure 2. Temperature dependence of magnetic moment of a Sn₉₀In₁₀ alloy by field cooling mode (FC curve) after quenched from annealing temperatures of 340 K and 380 K respectively.

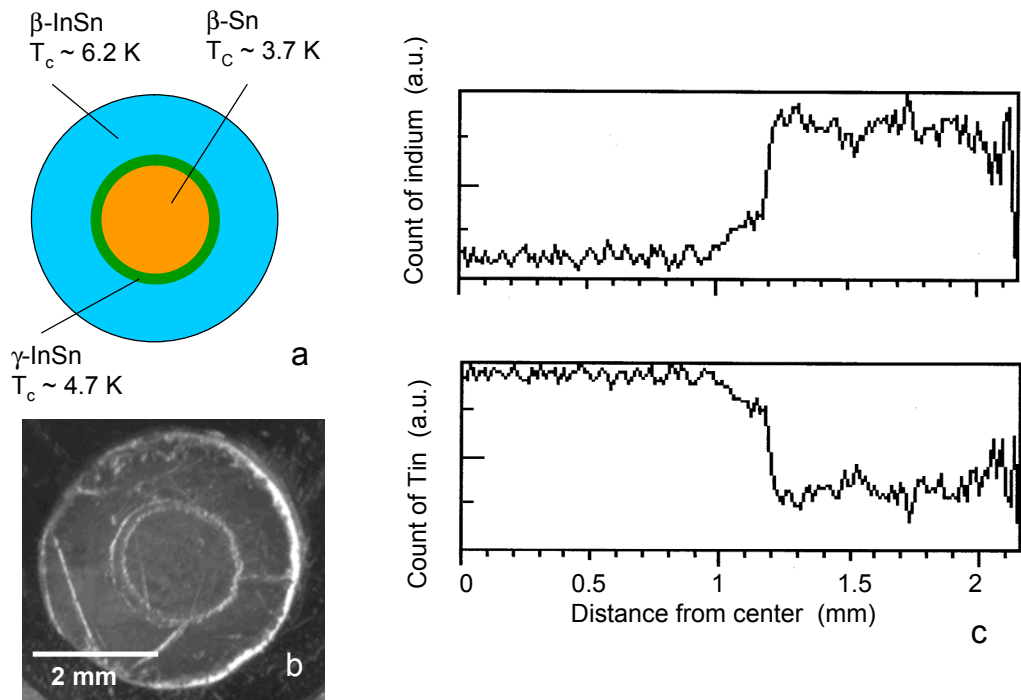


Figure 3. (a) Schematic of the phase distribution across the manufactured sample. (b) Optical macrograph reveals the interfaces between the three phases, (c) Composition profile clearly showing the three distinct phases.

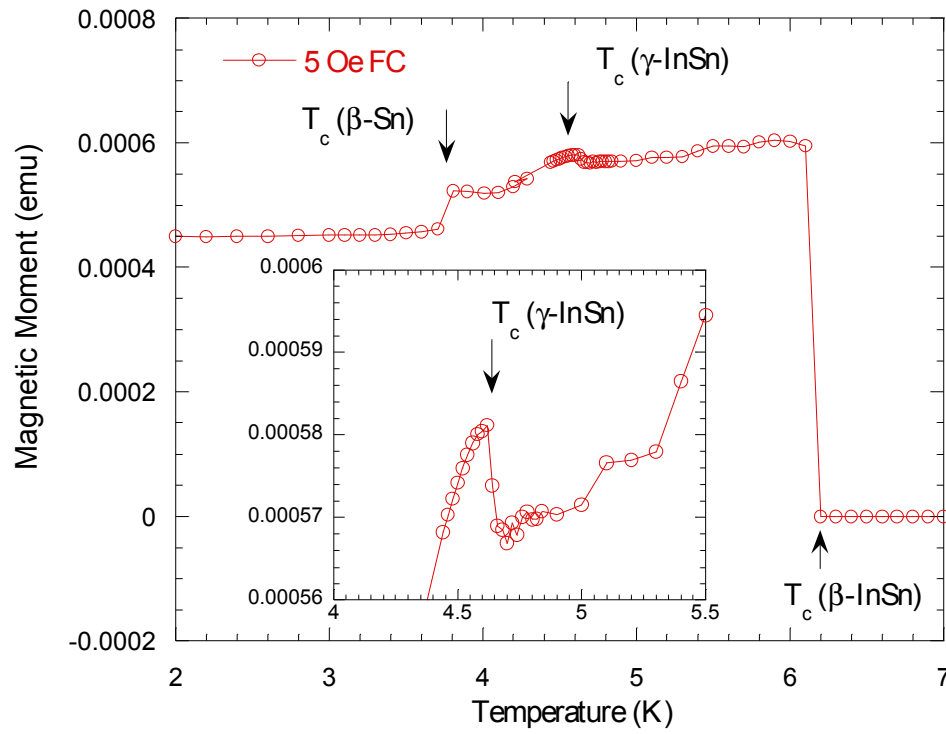


Figure 4. Temperature dependence of magnetic moment of a fabricated sample by field cooling mode (FC curve).